

breathing crack are smaller than those due to open cracks. Zabel and Rucker [14] investigated detection of fatigue cracks by vibration tests using an output-only covariance-based damage indicator. Hille et al. [15] performed an experimental fatigue test on a steel frame and applied output-only damage detection method assuming a linear state space model. Shaker and ambient excitations were studied. Bui et al. [16] performed system identification of a tubular structure under fatigue test assuming a linear state space model. Model updating approach was used for damage identification.

Producing a fatigue crack for laboratory tests is quite difficult and time-consuming. A numerical experiment using the finite element method can be used as an alternative solution. The number of numerical studies on vibration of cracked structures, especially simple beams, is large. Only a few studies are listed here. Friswell and Penny [17] reviewed different crack modelling strategies for SHM. The emphasis was in linear models with an open crack for a model updating application. It was claimed that the higher harmonics due to a breathing crack would be probably masked by noise. Ruotolo et al. [18] created a cracked beam element and performed non-linear simulations. Beam with a breathing crack was modelled as a bilinear oscillator by Chatterjee [2]. Waheed et al. [19] used a three-dimensional finite element model with contact elements to model a breathing crack in a rotating blade. Tondreau and Deraemaeker [20] suggested strain measurements for better damage localization, because strains are local properties and proportional to curvatures. Because of the local property, a large sensor network is needed, which can be obtained using fiber-optic sensors. Kullaa et al. [21] studied damage detection of a simulated two-dimensional beam with a breathing crack modelled with the finite element method.

In the present study, vibration of a three-dimensional structure with a breathing crack is analyzed. The structure is a hollow pipe used frequently in structures due to its high stiffness-to-weight property. The objective is to determine the smallest detectable crack using acceleration or strain measurements.

The paper is organized as follows. The damage detection algorithm is presented in Section 2. Modelling and simulation for data generation are studied in Section 3. The results of damage detection for a breathing crack are shown in Section 4. Finally, concluding remarks are given in Section 5.

2. DAMAGE DETECTION USING VIBRATION MEASUREMENTS

Fatigue damage is caused by alternating loading, such as vibrations. Vibration response can be measured using e.g. accelerometers, strain gauges, or laser. In civil engineering structures, the excitation is often difficult to measure. Therefore, damage has to be identified from response measurements only.

If the system is linear, the dynamic response $\mathbf{x}(t)$ of a linear system can be decomposed into contributions of the d lowest modes and the static correction term [22]:

$$\mathbf{x}(t) = \sum_{i=1}^d \phi_i q_i(t) + \left[\mathbf{K}^{-1} - \sum_{i=1}^d \mathbf{F}_i \right] \mathbf{B}f(t) \quad (1)$$

where ϕ_i is the mode shape vector of mode i and $q_i(t)$ is the response of mode i . The term in brackets is a constant matrix, where \mathbf{K} is the stiffness matrix of the system and \mathbf{F}_i is

$$\mathbf{F}_i = \frac{\phi_i \phi_i^T}{\phi_i \mathbf{K} \phi_i^T} \quad (2)$$

Vector $f(t)$ contains the load amplitude functions and \mathbf{B} is the load distribution matrix with the number of columns equal to the number of load amplitude functions. If the spatial distribution of the load does not vary with time and \mathbf{B} has r columns, the number of independent variables is $d + r$.

Let us assume that vibration is measured with a sensor network using simultaneous sampling. If the number of sensors is greater than $d + r$, the sensor network is redundant, and the signal of each sensor can be estimated using those of the remaining sensors in the network. A linear regression model is built for each sensor using the available data from the undamaged structure. Once there is crack or other damage, this model does not fit with the experimental data producing a larger error, which will then trigger an alarm.

Each observation \mathbf{x} is divided into predicted variables \mathbf{u} and the remaining variables \mathbf{v} :

$$\mathbf{x} = \begin{Bmatrix} \mathbf{u} \\ \mathbf{v} \end{Bmatrix} \quad (3)$$

with a partitioned mean vector $\boldsymbol{\mu}$ and data covariance matrix $\boldsymbol{\Sigma}$:

$$\boldsymbol{\mu} = \begin{Bmatrix} \boldsymbol{\mu}_u \\ \boldsymbol{\mu}_v \end{Bmatrix}, \quad \boldsymbol{\Sigma} = \begin{bmatrix} \boldsymbol{\Sigma}_{uu} & \boldsymbol{\Sigma}_{uv} \\ \boldsymbol{\Sigma}_{vu} & \boldsymbol{\Sigma}_{vv} \end{bmatrix} = \begin{bmatrix} \boldsymbol{\Gamma}_{uu} & \boldsymbol{\Gamma}_{uv} \\ \boldsymbol{\Gamma}_{vu} & \boldsymbol{\Gamma}_{vv} \end{bmatrix}^{-1} \quad (4)$$

where the precision matrix $\boldsymbol{\Gamma}$ is defined as the inverse of the covariance matrix $\boldsymbol{\Sigma}$ and is also written in the partitioned form. A linear minimum mean square error (MMSE) estimate for $\mathbf{u}|\mathbf{v}$ (\mathbf{u} given \mathbf{v}) is obtained by minimizing the mean-square error (MSE) and can be computed either using the covariance or precision matrix. If each variable is estimated in turn, the formulas based on the precision matrix result in a more efficient algorithm [23]. The expected values of the predicted variables are:

$$\hat{\mathbf{u}} = E(\mathbf{u}|\mathbf{v}) = \boldsymbol{\mu}_u - \boldsymbol{\Gamma}_{uu}^{-1} \boldsymbol{\Gamma}_{uv} (\mathbf{v} - \boldsymbol{\mu}_v) \quad (5)$$

and the covariance of the conditional distribution is

$$\text{cov}(\mathbf{u}|\mathbf{v}) = \boldsymbol{\Gamma}_{uu}^{-1} \quad (6)$$

The residuals for each variable are generated as follows.

$$\boldsymbol{\varepsilon} = \mathbf{u} - \hat{\mathbf{u}} \quad (7)$$

All residuals are standardized according to the training data. These standardized residuals are then subjected to principal component analysis (PCA). All samples, training and test data, are included in PCA in order to find the direction in the data space with the largest change, which is supposed to indicate damage. If the first principal component scores of the residuals are not normally distributed and the distribution is unknown, a generalized extreme value distribution can be used independently of the data distribution [24]. The scores are divided into subgroups (of size $n = 100$) and the subgroup minima and maxima are recorded. Extreme value distributions are identified for both the subgroup minima and maxima of the in-control samples (training data). The control limits are computed to these distributions by choosing the probability of exceedance (here 0.001). The extreme values are plotted on a control chart [25] to see if the test samples exceed the control limits thus indicating damage.

3. FINITE ELEMENT SIMULATIONS

3.1 Structure

The structure under investigation was a three-dimensional cantilever steel beam with a hollow circular cross-section. A standard profile was chosen with an outer diameter of $D = 101.6$ mm and wall thickness of $t = 3.6$ mm. The length of the beam was $L = 2.0$ m. The material properties were the following: Young's modulus $E = 209$ GPa, Poisson ratio $\nu = 0.30$, and density $\rho = 7850$ kg/m³.

The beam was modelled with eight-node solid elements with incompatible modes (element C3D8I in Abaqus). The model consisted of three parts (Figure 1): a long pipe with a length of 1.980 m having a relatively coarse mesh and two short parts, each with a length of 10 mm, having a dense mesh for more accurate crack modelling. The adjacent parts were connected using the automatic Tie property in Abaqus. In the dense mesh, there were two elements through the wall thickness, 104 elements along the circumferential direction, and 5 elements along the beam axis. In the coarse mesh, there was one element through the wall thickness, 52 elements along the circumferential direction, and 288 elements along the beam axis. Finally, the assembly consisted of 33,800 nodes and 17,056 elements. All displacement DOFs were constrained at the support.

The applicability of the element type and mesh was validated with static and modal analyses of the uncracked structure, for which exact results from the beam theory were available. The three-dimensional structure contained also several other modes typical for shell structures, for example radial modes. More information of the modelling can be found in [26].

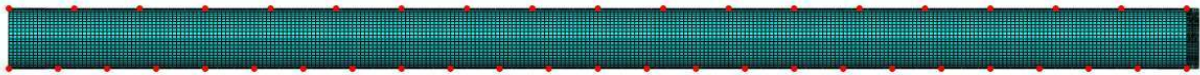


Figure 1: Finite element model of the structure. Sensor locations are also shown. The fixed support is at the right end and the crack is located at the top of the beam 10 mm left from the support.

3.2 Crack

The crack was located at the top of the beam, 10 mm from the fixed support between the two short parts symmetrically to the vertical neutral axis (Figure 2). The breathing crack was modelled by defining contact conditions between the crack surfaces. Abaqus general contact option was used to define the interaction between the crack surfaces. Frictionless contact was assumed in the tangential direction, and the Abaqus surface-to-surface option was used in the normal direction.

Simulations were performed for the undamaged and damaged structures with crack sizes of 0%, 7.7%, 13.5%, 25%, and 50% of the cross-sectional area (Figure 3). All cracks extended through the wall thickness. Corresponding open cracks were also analysed for comparison. For the breathing and open cracks, the models were identical, except for the contact definition, which was removed from the models with an open crack.

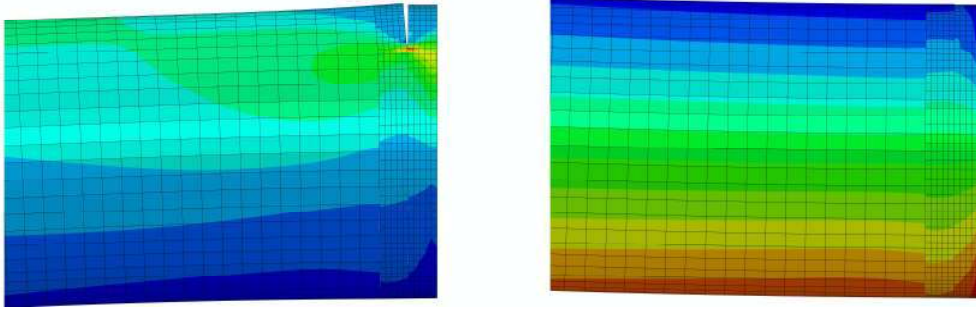


Figure 2: Breathing crack of size 25% of the cross-sectional area in open and closed positions with contours of longitudinal strains superimposed.

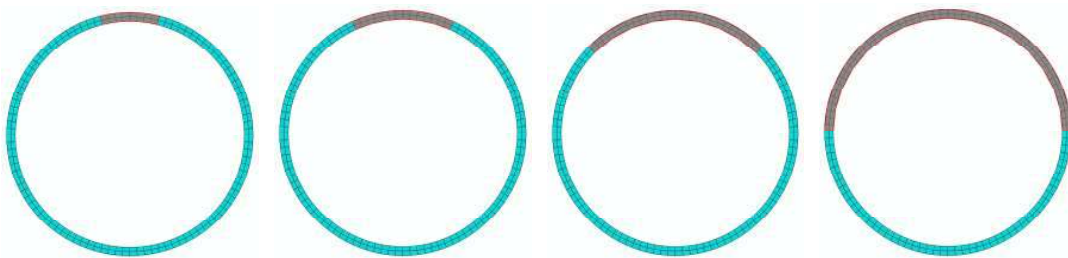


Figure 3: Cracks (dark) of 7.7%, 13.5%, 25%, and 50% of the cross-sectional area.

3.3 Excitation

The structure was excited by a pressure load uniformly distributed under the area of 12 elements at the free end of the beam (Figure 4). A different random loading function was generated for each simulation. The excitation was low-pass filtered below 2000 Hz before applying to the structure.

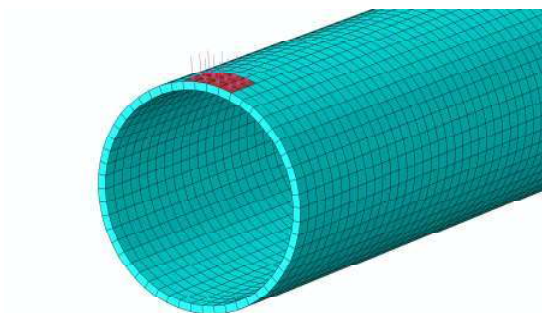


Figure 4: Load position.

3.4 Sensors

Accelerations and strains were measured at selected nodes at the bottom and at the top of the beam (Figure 1). The accelerometers measured vertical direction, while the strain sensors measured the normal strain in the beam direction. The bottom side consisted of 25 equidistant sensors and the top side 19 equidistant sensors of each type. All sensors were located in the

large part, so that the distance of the sensor closest to the crack was 10 mm. The furthest sensors were located at the free end of the beam. Measurements were acquired with a sampling frequency of 0.1 ms. Noise was added to all sensors so that on the average, the signal-to-noise ratio (SNR) of the network was 30 dB.

3.5 Simulation results

Simulations were carried out using explicit time integration. The simulation time was 0.5 s. Zero initial conditions were used. A very small time increment $2.0 \cdot 10^{-7}$ s had to be used for numerical stability. Damping was assumed zero, because introducing Rayleigh damping in the explicit integration would have decreased the stability limit of the time increment causing the computational time to increase considerably.

It should be noted that although the excitation was in the low frequency range, the contact behaviour could be a source of higher frequencies. Therefore, aliasing of the frequencies higher than half of the selected sampling frequency may have occurred. This is probably not an issue in SHM, because absolute frequency values are not needed.

Each simulation consisted of 5000 samples. The uncracked structure was simulated twice, while the cracked structure was simulated once with each crack size.

It was seen that the acceleration amplitudes increased during the whole simulation period. This was due to the fact that the damping was zero and vibration did not reach the steady state condition during the analysis period.

4. DAMAGE DETECTION OF A BREATHING CRACK

The first measurement (samples 1–5000) was used as the training data and also as the in-control data to design the control charts. Damage detection was done using four different sensor networks: (1) accelerometers at the top of the beam (crack side); (2) accelerometers at the bottom of the beam; (3) strain gauges at the top of the beam; and (4) strain gauges at the bottom of the beam. The number of sensors at the top and bottom of the beam was 19 and 25, respectively. The strain gauges and accelerometers were located at the same nodes. For each sensor network, the sensor numbering started from the free end of the beam.

4.1 Damage detection using acceleration sensors

First, all 19 accelerometers at the top of the beam were used for damage detection. The extreme value statistics (EVS) control chart for the first principal component of the residuals are plotted in Figure 5 left. All crack sizes could be detected with no false alarms. Crack localization was based on the largest relative error between the residual and the measurement signal. The crack was correctly localized close to sensor 19 (Figure 5 right).

For the 25 sensors at the bottom of the beam, the corresponding analysis was made, and the resulting control chart and the crack localization plot are shown in Figure 6. Again, all cracks could be detected with no false alarms, and damage was correctly localized to the closest sensor.

It can be seen from the control charts that the statistics increase with an increasing vibration amplitude. However, with the uncracked structure (measurements 1 and 2), the statistic remains constant. This is an indication that for the uncracked structure, the damage-sensitive feature is immune to the vibration amplitude, which is important in output-only approaches of SHM.

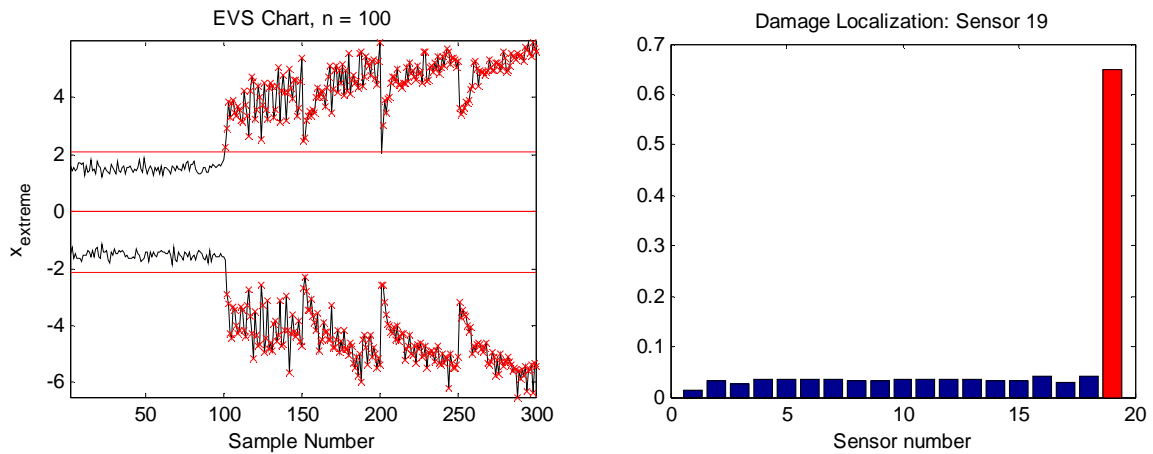


Figure 5: Left: EVS chart of the first PC scores of the top network with 19 accelerometers. Right: Damage localization.

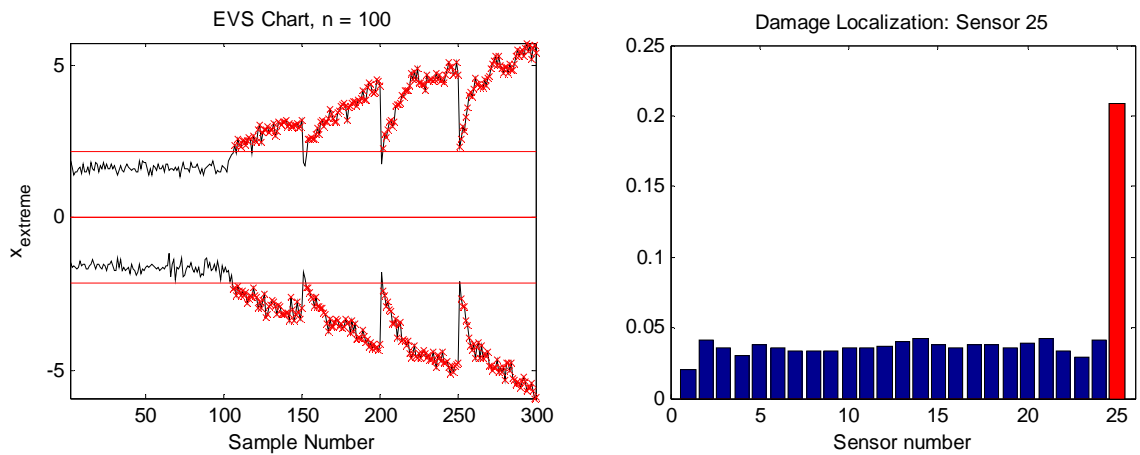


Figure 6: Left: EVS chart of the first PC scores of the bottom network with 25 accelerometers. Right: Damage localization.

4.2 Damage detection using strain sensors

Next, damage detection using strain sensors measuring the longitudinal strain on the surface of the pipe was studied. The sensor locations were the same as for the accelerometers.

For the 19 sensors on the top of the beam, the EVS control charts for the first principal component of the residuals of the data are plotted in Figure 7 left. For the 25 sensors at the bottom of the beam, the corresponding EVS chart is plotted in Figure 7 right.

It can be seen that breathing crack damage could be detected also with strain sensors, but the sensitivity to damage was smaller than that with accelerometers. Detection of the smallest crack was uncertain. Typically, the measurement error of strain gauges is larger than that of high-quality accelerometers, which also suggests preferring accelerometers to strain gauges in SHM. Crack localization failed in both cases.

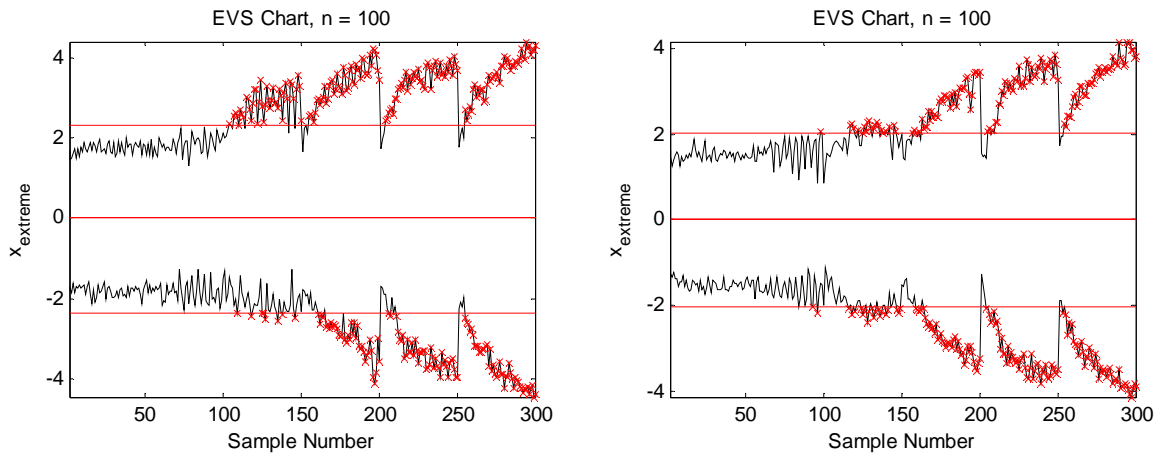


Figure 7: Left: EVS chart of the first PC scores of the top network with 19 strain gauges. Right: EVS chart of the first PC scores of the bottom network with 25 strain gauges.

5. CONCLUSIONS

Damage detection of a cantilevered pipe with a fatigue crack was studied using vibration measurements. Measurement data were simulated using a three-dimensional finite element model with a breathing crack subject to random excitation. The performance of acceleration and strain measurements using relatively dense sensor networks was studied.

The simulations showed that accelerations were more sensitive to damage than strains. It was seen that a breathing crack could be detected quite far from the sensor using vibration measurements. Damage localization was successful using accelerometers, but failed using strain gauges. An open crack proved to be very difficult to detect with the proposed algorithm [26].

Experimental verification is still needed, because there are several uncertainties in the modelling of the contact behaviour of a breathing crack. First, the crack sides were modelled as flat planes, which is not very realistic. Also, hard contact with no friction was assumed.

Damage detection was made in the time domain. No complex system identification was needed. The algorithm is eventually based on detecting changes in the mode shapes, but it is also able to detect non-linearity. In order to track the natural frequencies, the data could be time-shifted in order to take also the temporal correlation into account. In that case, steady state conditions may be needed.

REFERENCES

- [1] K. Worden, C.R. Farrar, J. Haywood, M. Todd, A review of nonlinear dynamics applications to structural health monitoring. *Structural Control and Health Monitoring*, **15**, 540-567, 2008.
- [2] A. Chatterjee, Crack detection in a cantilever beam using harmonic probing and free vibration decay. *Proceedings of the IMAC-XXVII, February 9-12, 2009 Orlando, Florida USA*.

- [3] C. Surace, R. Ruotolo, D. Storer, Detecting nonlinear behaviour using the volterra series to assess damage in beam-like structures. *Journal of Theoretical and Applied Mechanics*, **49**, 905-926, 2011.
- [4] S.L. Tsyfansky, V.I. Beresnevich, Detection of fatigue cracks in flexible geometrically non-linear bars by vibration monitoring. *Journal of Sound and Vibration*, **213**, 159-168, 1998.
- [5] F. Semperlotti, K.W. Wang, E.C. Smith, Localization of a Breathing Crack Using Super-Harmonic Signals due to System Nonlinearity. *American Institute of Aeronautics and Astronautics*, **47**, 2076-2086, 2009.
- [6] S. Benfratello, P. Cacciola, N. Impollonia, A. Masnata, G. Muscolino, Crack identification in a beam by measure of the response to white noise. *Proceedings of the 11th International Conference on Fracture*, Turin, Italy, 20-25 March, 2005.
- [7] V.K. Nguyen, O.A. Olatunbosun, A proposed method for fatigue crack detection and monitoring using the breathing crack phenomenon and wavelet analysis. *Journal of Mechanics of Materials and Structures*, **2**, 399-420, 2007.
- [8] S.M. Cheng, X.J. Wu, W. Wallace, Vibrational response of a beam with a breathing crack. *Journal of Sound and Vibration*, **225**, 201-208, 1999.
- [9] S. Loutridis, E. Douka, L.J. Hadjileontiadis, Forced vibration behaviour and crack detection of cracked beams using instantaneous frequency. *NDT & E International*, **38**, 411-419, 2005.
- [10] G. Yan, A. De Stefano, E. Matta, R. Feng, A novel approach to detecting breathing-fatigue cracks based on dynamic characteristics. *Journal of Sound and Vibration*, **332**, 407-422, 2013.
- [11] F. Vestroni, O. Giannini, P. Casini, Crack detection by nonlinear harmonic identification in beam structures. *Proceedings of the 9th International Conference on Structural Dynamics, EURO-DYN 2014*, A. Cunha, E. Caetano, P. Ribeiro, G. Müller (eds.), Porto, Portugal, 30 June - 2 July 2014, 2363-2369.
- [12] S. Vanlanduit, E. Parloo, P. Guillaume, Combined damage detection techniques. *Journal of Sound and Vibration*, **266**, 815-831, 2003.
- [13] T.G. Chondros, A.D. Dimarogonas, J. Yao, Vibration of a beam with a breathing crack. *Journal of Sound and Vibration*, **239**, 57-67, 2001.
- [14] V. Zabel, W. Rucker, Detection of a Fatigue Crack by Vibration Tests. *Proceedings of the IMAC-XXVII*, February 9-12, 2009 Orlando, Florida USA, Society for Experimental Mechanics.
- [15] F. Hille, Y. Petryna, W. Rucker, Subspace-based detection of fatigue damage on a steel frame laboratory structure for offshore applications. *Proceedings of the 9th International*

- Conference on Structural Dynamics, EUROODYN 2014, A. Cunha, E. Caetano, P. Ribeiro, G. Müller (eds.), Porto, Portugal, 30 June - 2 July, 2014, 3595-3602.
- [16] T.T. Bui, G. De Roeck, J. Van Wittenberghe, P. De Baets, W. De Waele, A modal approach to identify fatigue damage in threaded connections of large scale tubular structures. Proceedings of ISMA2010, International Conference on Noise and Vibration Engineering, P. Sas, B. Bergen (eds.), Leuven, Belgium, September 20-22, 2010, 795-808.
- [17] M.I. Friswell, J.E.T. Penny, Crack modelling for structural health monitoring. *Structural Health Monitoring: An International Journal*, **1**, 139-148, 2002.
- [18] R. Ruotolo, C. Surace, P. Crespo, D. Storer, Harmonic analysis of the vibrations of a cantilevered beam with a closing crack. *Computers & Structures*, **61**, 1057-1074, 1996.
- [19] S.O. Waheed, N.H. Mostafa, D.H. Jawad, Nonlinear dynamic characteristics of a simple blade with breathing crack using Ansys software. *World Journal of Mechanics*, **2011**, 21-30.
- [20] G. Tondreau, A. Deraemaeker, Damage localization in bridges using multi-scale filters and large strain sensor networks. Proceedings of ISMA2010, International Conference on Noise and Vibration Engineering, P. Sas, B. Bergen (eds.), Leuven, Belgium, September 20–22, 2010, 1477-1490.
- [21] J. Kullaa, K. Santaoja, A. Eymery. Vibration-based structural health monitoring of a simulated beam with a breathing crack. *Key Engineering Materials Vols. 569-570, Damage Assessment of Structures X*. Trans Tech Publications, Switzerland, 1093-1100, 2013.
- [22] R.W. Clough, J. Penzien, *Dynamics of structures*. 2nd edition, McGraw-Hill, New York, (1993).
- [23] J. Kullaa, Sensor validation using minimum mean square error estimation. *Mechanical Systems and Signal Processing*, **24**, 1444-1457, 2010.
- [24] K. Worden, D. Allen, H. Sohn, C.R. Farrar, Damage detection in mechanical structures using extreme value statistics. In: *SPIE Proceedings, Vol. 4693, 9th Annual International Symposium on Smart Structures and Materials*, San Diego, CA, 2002, 289-299.
- [25] D.C. Montgomery, *Introduction to statistical quality control*. 3rd edition, John Wiley, New York (1997).
- [26] M. Miettinen. *Fatigue Crack Modeling for Damage Detection*. Bachelor Thesis at Helsinki Metropolia University of Applied Sciences, 2016. [In Finnish.]